Convergence of the solution of the continuum discretized coupled channels method

R. A. D. Piyadasa
Department of Mathematics, University of Kelaniya, Kelaniya, Sri Lanka

M. Kawai and M. Kamimura
Department of Physics, Kyushu University, Fukuoka 812-8581, Japan

M. Yahiro
Department of Physics and Earth Sciences, University of Ryukyus, Nishihara-cho, Okinawa 903-0213, Japan
(Received 21 April 1999; published 8 September 1999)

The validity of the method of continuum discretized coupled channels (CDCC) is numerically tested and confirmed for a realistic example of $d+^{58}$Ni scattering at 80 MeV. Elastic and breakup S-matrix elements, calculated with the CDCC method, numerically converge as the model space is extended, viz., the internal angular momentum of the proton-neutron pair and the matching radius are increased. Two methods of discretization, the average method and midpoint method, of the continuum of the internal linear momentum of the p-n pair are tested and found to yield the same results. [S0556-2813(99)00810-9]

PACS number(s): 24.10.Eq, 25.45.−z

I. INTRODUCTION

The method of continuum discretized coupled channels (CDCC) has been successful in describing nuclear reactions involving breakup processes of weakly bound projectiles [1,2], and its theoretical foundation has been a subject of extensive studies [1–10]. The CDCC method is concerned with a three-body system comprised of two fragments into which the projectile is breakable and a target nucleus which is assumed to be an inert core. One assumes a three-body Hamiltonian H for the system comprising the kinetic energies of the three particles and the interaction potentials between all pairs of particles in the system. In the case of a nuclear reaction such as the one we investigate in the present paper, one takes optical potentials for the interaction between the target and each of the fragments of the projectile. The CDCC method is a practical method of solving the three-body Schrödinger equation $(H-E)\Psi=0$. In the CDCC method, Ψ is expanded in the basis of the complete set of eigenfunctions of the internal Hamiltonian of the projectile. Each eigenfunction defines a channel, and is characterized by the orbital angular momentum, l and the linear momentum k of relative motion of the fragments if the state is in the continuum, and the principal quantum number n if it is a bound state. The unknown coefficient of the expansion is the wave function of relative motion between the projectile and the nucleus and is a function of the relative coordinate of the channel, viz., the coordinate $\mathbf{R}$ of the center-of-mass of the projectile relative to that of the target nucleus. A set of coupled equations for the wave functions of the relative motion of the channels is derived from the three-body Schrödinger equation. It is impossible to solve the coupled channels equations exactly since the breakup states have l ranging from 0 to infinity, and k is continuous so that a continuously infinite number of channels are coupled in the equations. In order to overcome this difficulty, the following two approximations are made in the CDCC method.

The first approximation is the truncation of k and l by $k \leqslant k_m$ and $l \leqslant l_m$, and the setting of the the asymptotic outgoing wave boundary condition at $R=R_m$. We call this approximation the model space approximation. It is justified if the CDCC solution converges to the exact one as the model space is extended.

The second approximation is the discretization of the k continuum. Two methods of discretization have been used so far, the average (Av) method [3] and the midpoint (Mid) method [9]. It is the former method that is widely used in practice and is examined in the present paper. In these methods, the k continuum is divided into a finite number of bins, and the internal states within each bin are represented by a single wave function. For the validity of this approximation it is necessary that the result of the calculations converge as the number of the bins is increased and consequently the sizes of the bins are decreased, and that it be independent of the method of discretization.

The validity of the discretization was examined in Ref. [3] with the Av method in which the internal wave functions of the continuous breakup states within each bin were averaged to get the representative wave function of the bin. Calculated breakup S-matrix elements converged as the common size of the bin, Δ, was decreased with k_m kept fixed. The Av method, however, was criticized [7] in that it suppressed the channel coupling potentials between breakup states at large R. We have then examined the numerical convergence of the CDCC solution with the Mid method [9] in which the continuous breakup states in each bin were simply represented by a breakup state wave function at a midpoint of the bin. Convergence was clearly seen as Δ decreased with k_m kept fixed. This result was free from the criticism mentioned above since the original asymptotic form of the internal wave functions was retained in the representative one and, hence, no suppression of the coupling potentials between breakup states at large R.

The question of crucial importance is whether the CDCC solution, even though it numerically converges as the model space is enlarged, converges to the correct solu-

tion of the three-body problem. This problem has been addressed in Ref. [10]. It has been shown that the CDCC solution is first-order approximation to a set of distorted-wave Faddeev equations [11], and corrections to the CDCC solution can be estimated and shown to decrease as the model space is extended, unless incoming waves are generated in breakup channels at $R \geqslant R_m$. If incoming waves are generated there, they go back to the inner region $R < R_m$ in which coupling potentials between breakup channels are strong and much affect the CDCC solution in that region. A theoretical foundation of the CDCC solution, therefore, is the assumption that few incoming waves are generated at $R \geqslant R_m$ in breakup channels. An aim of this paper is to verify this assumption with numerical calculations.

The theoretical consideration of Ref. [10] makes no mention of how fast the convergence is with respect to the extension of the model space. If the convergence is too slow, the CDCC solution is not useful in practice. So we have to examine how fast the convergence is. In Ref. [3], the CDCC solution was found to converge at a reasonable size of the model space. The examination, however, used the Av method for discretization. Another aim of this paper is to reexamine the convergence with the Mid method for discretization and show that the convergence is realized at a reasonable size of the model space.

The last aim of the present paper is to test whether the two methods of discretization give the same results. In practice, the Av method is more convenient than the Mid method, since the Av method requires less numerical works than the Mid method.

The present paper gives a full account of our investigations concerning the validity and the practicality of the CDCC method, together with discussions in terms of the behavior of the channel coupling potentials. As the test case, we take the same realistic example of deuteron scattering and breakup on ^{58}Ni at 80 MeV as in the previous work [3]. The construction of this paper is as follows. In Sec. II, we recapitulate the method of CDCC and its assumptions. In Sec. III, our method of calculation is presented. In Sec. IV, numerical results are presented, and Sec. V is devoted to a summary and discussion.

II. METHOD OF CDCC

We consider a reaction initiated by a deuteron (d) impinging on a target nucleus (A). In the CDCC method, it is assumed that the reaction in the three-body system comprising A and the neutron (n) and proton (p) pair in d can be described by a model Hamiltonian

$$H = K_r + K_R + V_{np}(\mathbf{r}) + U_n(\mathbf{R} - \mathbf{r}/2) + U_p(\mathbf{R} + \mathbf{r}/2) + U_c(R). \tag{2.1}$$

Here $V_{np}(\mathbf{r})$ is the interaction between n and p. The vector $\mathbf{r}$ is a coordinate of p relative to n, and $\mathbf{R}$ is the coordinate of the center of mass of the p-n pair relative to A. The interaction $U_p(\mathbf{R}+\mathbf{r}/2)$ $[U_n(\mathbf{R}-\mathbf{r}/2)]$ between p (n) and A is assumed to be the central nuclear part of the proton [neutron] optical potential at half the deuteron incident energy, $E_d/2$. We approximate the Coulomb potential between p and A by that between d and A, $U_c(R)$, neglecting its effect on the internal motion of the n-p pair. The operators K_r and K_R are the kinetic energies associated with $\mathbf{r}$ and $\mathbf{R}$.

In the CDCC method, the three-body wave function Ψ_{JM}, associated with the total angular momentum J and its projection M on the z axis, is expanded as

$$\Psi_{JM}(\mathbf{r},\mathbf{R}) = \Phi_0(r) Y_{00}(\Omega_r) Y_{JM}(\Omega_R) g_J(P_0,R)/R + \sum_{l=0}^{\infty} \sum_{L} [Y_l(\Omega_r) \otimes Y_L(\Omega_R)]_{JM} \times \int_0^{\infty} \Phi_l(k,r) g_{lLJ}(P,R) dk/R \tag{2.2}$$

in an orthonormal basis set of the internal wave functions of the p-n pair, Φ, comprising the ground state wave function $\Phi_0(r)$ and the breakup state wave functions $\Phi_l(k,r)$, characterized by the linear momentum k and the angular momentum l of relative motion between p and n, both ranging from zero to infinity. We assume that the deuteron ground state is an s state so that $l=0$. The $\Phi_l(k,r)$ are normalized to a δ function in k. The coefficients $g_{lLJ}(P,R)$ of the expansion describe the motion of a broken-up p-n pair in the state $\Phi_l(k,r)$ relative to A. The linear and orbital angular momenta of the motion are denoted by P and L, respectively, and the total angular momentum by J. Here J is given by a vector coupling of the angular momenta l and L. Since we assume $l=0$ for the deuteron ground state, we obtain $J=L$ for the elastic channel. We denote the linear momentum of the incident deuteron by P_0. The momenta P_0 and P satisfy the total energy conservation

$$E = \frac{\hbar^2 P^2}{2\mu} + \frac{\hbar^2 k^2}{m_N} = \frac{\hbar^2 P_0^2}{2\mu} + \epsilon_0, \tag{2.3}$$

where E is the total energy of the system, ϵ_0 is the binding energy of d, m_N is the nucleon mass, and $\mu = m_N \times 2A/(A+2)$ is the reduced mass.

As the first assumption of the CDCC method, the sum over l is truncated by $l \leqslant l_m$ and the k integral by $k \leqslant k_m$. We simply take k_m common to all l in the present paper. As the second assumption, the truncated k continuum $[0, k_m]$ is discretized as follows. The truncated k continuum $[0, k_m]$ is first divided into a finite number N of bins, $[0,k_1]$, $[k_1,k_2]$, ..., $[k_i,k_{i+1}]$, ..., $[k_{N-1},k_N]$, each with a common width $\Delta = k_{i+1} - k_i = k_m/N$. The wave functions of the continuous breakup states in the ith bin are replaced by a wave function $\hat{\Phi}_{il}(r)$. Two methods have been used to define $\hat{\Phi}_{il}(r)$, the average (Av) method and midpoint (Mid) method. The $\hat{\Phi}_{il}(r)$ are defined in each method as

$$\hat{\Phi}_{il}(r) = \frac{1}{\sqrt{\Delta}} \int_{k_{i-1}}^{k_i} \Phi_l(k,r) dk \quad \text{(for Av)}, \tag{2.4}$$

$$\hat{\Phi}_{il}(r) = \sqrt{\Delta} \Phi_l(\bar{k}_i, r) \quad \text{(for Mid)}, \tag{2.5}$$

where $\overline{k_i}=(k_i+k_{i-1})/2$. The $\hat{\Phi}_{ilm}(\mathbf{r})$ satisfy

$$\int \hat{\Phi}^*_{ilm}(\mathbf{r})\hat{\Phi}_{i'l'm'}(\mathbf{r})d\mathbf{r}=\delta_{ii'}\delta_{ll'}\delta_{mm'} \quad \text{(for Av)}, \tag{2.6}$$

$$\int \hat{\Phi}^*_{ilm}(\mathbf{r})\hat{\Phi}_{i'l'm'}(\mathbf{r})d\mathbf{r}=\Delta\,\delta_{ll'}\delta(\overline{k_i}-\overline{k_{i'}})\delta_{mm'} \quad \text{(for Mid)}, \tag{2.7}$$

where $\hat{\Phi}_{ilm}(\mathbf{r})=\hat{\Phi}_{il}(r)Y_{lm}(\Omega_r)$. Under the two assumptions described above, Ψ_{JM} takes the form

$$\Psi_{JM}\approx\hat{\Phi}_0(\mathbf{r},\Omega_R)\hat{g}_J(P_0,R)/R + \sum_{l=0}^{l_m}\sum_{L}\sum_{i=1}^{N}\hat{\Phi}_\gamma(\hat{k}_i,\mathbf{r},\Omega_R)\hat{g}_\gamma(\hat{P}_i,R)/R, \tag{2.8}$$

where

$$\hat{\Phi}_0(\mathbf{r},\Omega_R)=\Phi_0(r)Y_{00}(\Omega_r)Y_{JM}(\Omega_R), \tag{2.9}$$

$$\hat{\Phi}_\gamma(\hat{k}_i,\mathbf{r},\Omega_R)=\hat{\Phi}_{il}(r)[Y_l(\Omega_r)\otimes Y_L(\Omega_R)]_{JM} \quad \text{for} \quad \gamma=(i,l,L,J,M) \tag{2.10}$$

and

$$\hat{g}_J(P_0,R)=g_J(P_0,R), \tag{2.11}$$

$$\hat{g}_\gamma(\hat{P}_i,R)=\sqrt{\Delta}g_\gamma(\hat{P}_i,R) \quad \text{for} \quad \gamma=(i,l,L,J,M). \tag{2.12}$$

The $\hat{k}_i$ are defined as $\hat{k}_i^2=\overline{k_i^2}+\Delta^2/12$ for the Av method [1] and $\hat{k}_i=\overline{k_i}$ for the Mid method. The momenta $\hat{k}_i$ and $\hat{P}_i$ satisfy the total energy conservation $E=\hbar^2\hat{P}_i^2/(2\mu)+\hbar^2\hat{k}_i^2/m_N$.

Unknown coefficient functions $\hat{g}_\gamma(\hat{P}_i,R)$ are determined by a set of coupled channels equations:

$$\left[\frac{d^2}{dR^2}-\hat{P}_i^2-\frac{L(L+1)}{R^2}-\frac{2\mu}{\hbar^2}V_{\gamma\gamma}(R)\right]\hat{g}_\gamma(\hat{P}_i,R) = \sum_{\gamma'\neq\gamma}\frac{2\mu}{\hbar^2}V_{\gamma\gamma'}(R)\hat{g}_{\gamma'}(\hat{P}_i,R) \tag{2.13}$$

for all γ including the elastic channel $\gamma=(0,0,J,J,M)$, for which $\hat{P}_0=P_0$. Equation (2.13) is the basic equation of CDCC method. The coupling potentials $V_{\gamma\gamma'}(R)$ are defined by

$$V_{\gamma\gamma'}(R)=\langle\hat{\Phi}_\gamma|U_p(\mathbf{R}+\mathbf{r}/2)+U_n(\mathbf{R}-\mathbf{r}/2)|\hat{\Phi}_{\gamma'}\rangle, \tag{2.14}$$

where the angular brackets stand for integrations over $\mathbf{r}$ and Ω_R, the angular part of $\mathbf{R}$. The $V_{\gamma\gamma'}(R)$ and the $\hat{g}_\gamma(\hat{P}_i,R)$ are independent of M since H is rotationally invariant. The set of coupled equations is solved under the asymptotic boundary condition [11]

$$\hat{g}_\gamma(\hat{P}_i,R)\sim u_L^{(-)}(\hat{P}_i,R)\,\delta_{\gamma,0}-\sqrt{\frac{\hat{P}_i}{\hat{P}_0}}S_{\gamma,0}u_L^{(+)}(\hat{P}_i,R), \tag{2.15}$$

where $u_L^{(-)}(\hat{P}_i,R)$ and $u_L^{(+)}(\hat{P}_i,R)$ are incoming and outgoing Coulomb wave functions with momentum $\hat{P}_i$ and $S_{\gamma,0}$ is the S-matrix element for a transition $0\rightarrow\gamma$, where 0 stands for the initial channel. At large R, $V_{\gamma\gamma}(R)$ between discretized breakup states decreases as R^{-4} for the Av method and R^{-2} for the Mid method, while the original coupling potentials between continuous breakup states do as R^{-2}. The CDCC calculations made so far for analyzing experimental data used the Av method. Asymptotic boundary conditions therefore can be set at a matching radius R_m of 30 fm or so, because of the fast damping of the Av coupling potentials. This, however, ought to be verified by showing that the same S-matrix elements are obtained with the Mid method in which the damping of the coupling potentials is much slower.

The assumptions made in the CDCC method are summarized as follows. The first assumption is the sufficiency of the model space defined with three types of truncations: (i) truncation of l by a maximum l_m, (ii) truncation of k by a maximum k_m, and (iii) setting the asymptotic outgoing wave boundary condition at $R=R_m$. The second assumption is (iv) discretization of the truncated k continuum $[0,k_m]$, by either the Av or Mid method. A set of coupled integral equations derived from the coupled differential equations (2.13) has compact kernels, owing to the model space truncation [10] even before the discretization. In this sense, the model space truncation is more basic than the discretization (iv). It is also shown in Ref. [10] that the CDCC solution tends to the exact solution as the model space is extended, provided (I) that no incoming wave is generated at $R>R_m$ by long ranged coupling potentials between breakup channels. Truncation (iii) is only justified if assumption (I) is valid. We test the truncations (i) and (iii), together with assumption (I), setting $k_m=1.0$ fm^{-1} as in Ref. [3]. Truncation (ii) is not examined in this paper since the previous test [3] confirmed its validity. We also investigate which of the Av and Mid methods is more practical as the method of discretization, (iv).

III. METHOD OF CALCULATION

We use the method of Ichimura *et al.* [12] to solve the coupled channels equations (2.13) since it is quite effective for long ranged coupling potentials. In that method, $\hat{g}_\gamma(\hat{P}_i,R)$ is expressed as

$$\hat{g}_\gamma(\hat{P}_i,R)=a_\gamma(R)f_\gamma(R)+a_\gamma^{(+)}(R)U_\gamma{}^{(+)}(R), \tag{3.1}$$

where $f_\gamma(R)$ and $U_\gamma^{(+)}(R)$ are regular and outgoing wave solutions of uncoupled Schrödinger equations with the diagonal potentials

$$\left[\frac{d^2}{dR^2}-\hat{P}_i^2-\frac{L(L+1)}{R^2}-\frac{2\mu}{\hbar^2}V_{\gamma\gamma}(R)\right]U_\gamma(R)=0, \quad (3.2)$$

where $U_\gamma(R)$ is either $f_\gamma(R)$ or $U_\gamma^{(+)}(R)$. The coefficients $a_\gamma(R)$ and $a_\gamma^{(+)}(R)$ satisfy the coupled differential equations

$$\frac{d}{dR}a_\gamma(R)=\frac{2\mu}{\hbar\hat{P}_\gamma}\sum_{\gamma'}\{[U_\gamma^{(+)}(R)V_{\gamma\gamma'}(R)f_{\gamma'}(R)]a_{\gamma'}(R) + [U_\gamma^{(+)}(R)V_{\gamma\gamma'}(R)U_{\gamma'}^{(+)}(R)]a_{\gamma'}^{(+)}(R)\}, \quad (3.3)$$

$$\frac{d}{dR}a_\gamma^{(+)}(R)=-\frac{2\mu}{\hbar\hat{P}_\gamma}\sum_{\gamma'}\{[f_\gamma(R)V_{\gamma\gamma'}(R)f_{\gamma'}(R)]a_{\gamma'}(R) + [f_\gamma(R)V_{\gamma\gamma'}(R)U_{\gamma'}^{(+)}(R)]a_{\gamma'}^{(+)}(R)\}, \quad (3.4)$$

and subject to the boundary conditions $a_\gamma(\infty)=\delta_{\gamma,0}$ and $a_\gamma^{(+)}(0)=0$. In actual calculations, however, the boundary condition for a_γ is set at $R=R_m$ instead of $R=\infty$. The coupled equations are solved iteratively starting from $a_\gamma^{(+)}(R)=0$ at all R. The resultant S-matrix elements are given by

$$S_{\gamma,0}=\left[S_0\delta_{\gamma,0}+2i\sqrt{\frac{\hat{P}_0}{\hat{P}_i}}a_\gamma^{(+)}(R_m)\right], \quad (3.5)$$

where S_0 is the S-matrix element for elastic scattering due to the potential $V_{00}(R)$. The S-matrix elements depend on R_m, but the R_m dependence is very weak, as shown in Sec. IV. In the present test, we extend l_m up to 8, R_m up to 90 fm, and N up to 20, while we keep $k_m=1$ fm^{-1} as mentioned in Sec. II.

IV. NUMERICAL RESULTS

The results of our test concerning two assumptions, the model space truncation and the discretization of the k continuum, for the case of $d+^{58}$Ni are presented in this section. We use the Becchetti-Greenlees [13] optical potentials for the neutron- and proton-nucleus interaction at half the deuteron incident energy, and neglect spins.

A. Discretization of the k continuum

In order to see how S-matrix elements depend on the method of discretization, we calculate breakup S-matrix elements $S(k)$ with both the Av and Mid methods in the identical model space with $k_m=1$ fm^{-1}, $R_m=30$ fm, and $l_m=0$, for N ranging from $N=5$ to $N=20$. Figure 1, quoted from Ref. [9], shows $S(k)$ at $E_d=80$ MeV and $J=17$, which is the grazing angular momentum, for four cases of $N=5$, 8, 12, and 20. As shown in the figure, $S(k)$ calculated with both the Av and Mid method converge to the same values at $N=12$. The same agreement is also seen for elastic S-matrix elements at much smaller N; in the case of $N=5$ and $J=17$, for example, the absolute value of the element is 0.6254 for the Av method and 0.6252 for the Mid method. It is clear that the Av method converges faster than the Mid method except k near k_m. The slow convergence of the Av method at k near k_m does not matter much in calculating breakup cross sections since the breakup S-matrix elements themselves are small for such k.

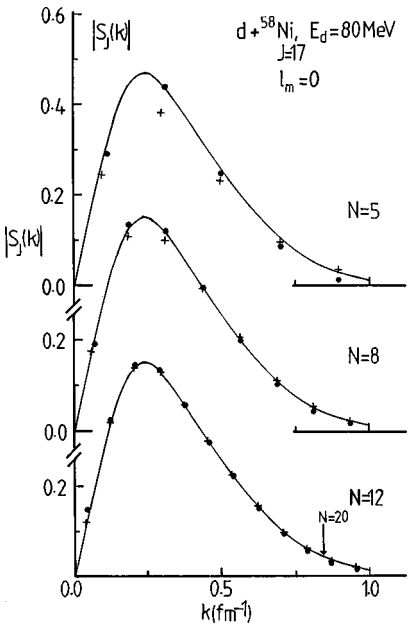

FIG. 1. The modulus of the S-matrix elements of breakup processes, $S(k)$, in $d+^{58}$Ni at 80 MeV. These are calculated by the CDCC method with Av (●) and Mid (+) discretizations with $N=5$, 8, 12, and 20. The solid lines correspond to the result of the Mid method with $N=20$. R_m is taken at 30 fm.

The superiority of the Av method to the Mid method in the convergence may be understood by the mean value theorem

$$\int_{k_i}^{k_{i+1}} g_\gamma(P,R)\Phi_\gamma(k,\mathbf{r},\Omega_R)dk = g_\gamma(\overline{P}_i,R)\int_{k_i}^{k_{i+1}}\Phi_\gamma(k,\mathbf{r},\Omega_R)dk, \quad (4.1)$$

where $\overline{P}_i$ satisfies $P(k_{i+1})<\overline{P}_i<P(k_i)$, which is true unless $\Phi_\gamma(k,\mathbf{r},\Omega_R)$ changes the sign within $[k_i,k_{i+1}]$. The right-hand side of Eq. (4.1) is $\sqrt{\Delta}g_\gamma(\overline{P}_i,R)\hat{\Phi}_\gamma(\hat{k}_i,\mathbf{r},\Omega_R)$, which is nothing but Av discretization if $\overline{P}_i=\hat{P}_i$. Since $dP(k)/dk=-2\mu k/[m_N P(k)]$ because of $E=\hbar^2P^2/(2\mu)+\hbar^2k^2/m_N$, $P(k)$ changes little over the interval $[k_i,k_{i+1}]$ if $k\ll P(k)$; hence $\overline{P}_i\approx\hat{P}_i$ except k near k_m. The Av discretization is thus justified.

In the Mid method, the left-hand side of Eq. (4.1) is approximated by $\sqrt{\Delta}g_\gamma(\hat{P}_i,R)\Phi_\gamma(\overline{k}_i,\mathbf{r},\Omega_R)$. For the validity

TABLE I. Convergence of the elastic S-matrix element with respect to increasing l_m at the grazing angular momentum $J=17$ for the system $d+{}^{58}$Ni at 80 MeV. Parameters taken are $R_m=30$ fm and $k_m=1$ fm^{-1}. Mid discretization is used with $N=8$.

l_m	$\lvert S^J_{\rm el}\rvert$	Phase (deg)
0	0.6242	24.4
2	0.5945	20.1
4	0.5956	19.9
6	0.5954	19.9

of this approximation, not only $g_\gamma(P,R)$ but also $\Phi_\gamma(k,\mathbf{r},\Omega_R)$ change little over the interval $[k_i,k_{i+1}]$. This condition is satisfied only for Δ smaller than that in the Av method. Thus, the Av method is more practical than the Mid method.

B. Model space truncation

The model space truncation is tested mainly with Mid discretization. As mentioned in Sec. II, this truncation is composed of three types of truncations; (i) truncation of l, (ii) truncation of k, and (iii) setting the asymptotic boundary condition at a finite value of R_m.

First, we test truncation (i). Table I shows rapid convergence of elastic S-matrix elements with respect to increasing l_m, at the grazing angular momentum $J=17$, which gives the largest contribution to the breakup cross section. In comparison, the $l=8$ breakup, for example, has a contribution of less than 0.04%. The breakup up to $l=2$ is sufficient for practical purposes.

Breakup S-matrix elements are much more sensitive to increasing l than the elastic S-matrix elements since l in the final state is not restricted as in the case of elastic scattering. In order to minimize numerical errors, we use the Av method in this part of our test. As shown in Figs. 2–5, breakup S-matrix elements converge at $l_m=6$ with $R_m=60$ fm fixed.

Next, we test truncation (iii). Since the Mid coupling potentials decay as R^{-2}, it is not obvious whether we can set the asymptotic boundary condition at a reasonable value of R_m. For $l_m=6$ and $J=17$, we, therefore, examine the validity of it for elastic S-matrix elements. The elastic S-matrix element calculated with the Mid method has modules 0.5954 and phase 19.9° at $R_m=30$ fm. These values remain unchanged even when R_m is increased up to 90 fm, as shown in Table II. The reason for this result is well understood in terms of the coefficient functions $a_\gamma(R)$ and $a^{(+)}_\gamma(R)$ of Eq. (3.1). We examine the behaviors of $a^{(+)}_\gamma(R)$ in the neighborhood of R_m set at 80 fm where the potential tails are negligibly small. Figure 6 is shown for the case of $J=17$, $l_m=0$, and $N=12$. It presents the ratio $\rho_\gamma=\lvert a_\gamma(R)/a^{(+)}_\gamma(R)\rvert$ for k_3, at which $\lvert S(k)\rvert$ is almost peaked, and for k_{12} close to k_m. The $\rho_\gamma(R)$ drop sharply as R increases. For k_3, or for the breakup channel $i=3$, it is about 0.4% near $R=20$ fm. For k_{12}, or for $i=12$, it is somewhat large, but still less than 3% at 20 fm. The outgoing wave boundary condition is thus satisfied within the accuracy of practical interest. This means that few incoming waves, of which $a_\gamma(R)$ is the amplitude,

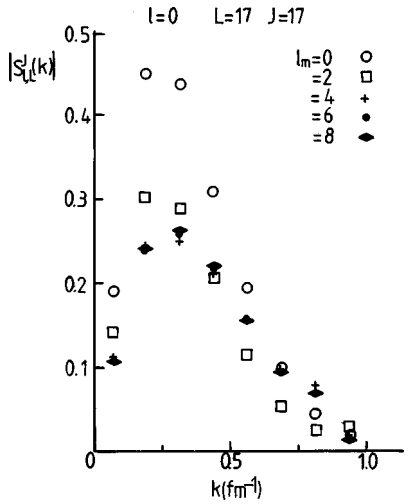

FIG. 2. Discretized S-matrix elements to s-wave breakup states with $J=17$ and $L=17$. These are calculated by the Av method. Here l_m varies from 0 to 8 through even values, while R_m is fixed at 60 fm. The symbols ○, □, +, ●, and ◇ correspond to $l_m=0$, 2, 4, 6, and 8, respectively.

are generated at $R\gtrsim 30$ fm in breakup channels. The validity of the asymptotic outgoing wave boundary condition for the channel $i=3$ is understandable, because even the diagonal potential which is the biggest among coupling potentials between breakup channels is a slowly varying function of R and is much smaller at $R\gtrsim 30$ fm than the asymptotic kinetic energy, $\hbar^2\hat{P}_i^2/2\mu$ [9]. For $i=12$, in contrast, this condition is not well satisfied, since the corresponding kinetic energy is quite small for the channel. However, the diagonal potential is still a slowly varying function of R especially at $R\gtrsim 30$ fm, and therefore produces few incoming waves there [14].

We next examine the behavior of $a^{(+)}_\gamma(R)$ as a function of R. Figure 7 shows the results for the case of $J=17$, $l_m=0$,

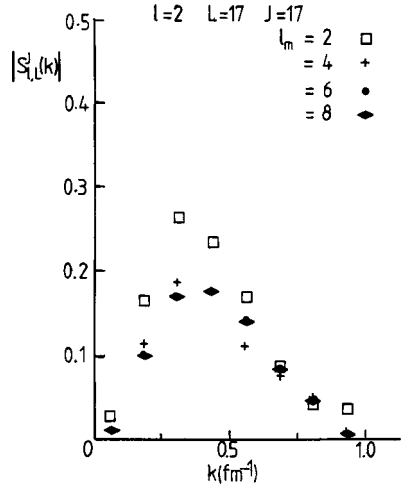

FIG. 3. Discretized S-matrix elements to d-wave breakup states with $J=17$ and $L=17$. These are calculated by the Av method. Here l_m varies from 0 to 8 through even values, while R_m is fixed at 60 fm. The symbols □, +, ●, and ◇ correspond to $l_m=2$, 4, 6, and 8.

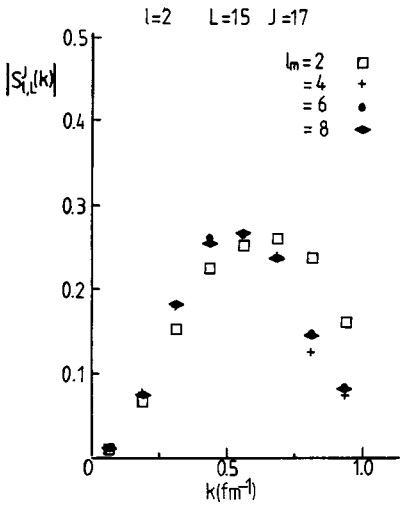

FIG. 4. Discretized breakup *S*-matrix elements to *d*-wave breakup states with $J=17$ and $L=15$. These are calculated by the Av method. Here l_m varies from 0 to 8 through even values, while R_m is fixed at 60 fm. The symbols □, +, ●, and ◇ correspond to $l_m=2$, 4, 6, and 8.

and $N=12$. Rapid convergence of $a_\gamma^{(+)}(R)$ is seen for its elastic component $i=0$ and breakup components $i=3$ and $i=12$. For $i=12$, $a_\gamma^{(+)}(R)$ shows a small slow convergence, but is practically independent of R for $R\gtrsim 30$ fm. This implies that almost all outgoing waves are generated at $R\lesssim 30$ fm and few outgoing waves are newly generated at $R\gtrsim 30$ fm. The same test for the same J and k_m is carried out for different l_m and N, i.e., $l_m=2$ and $N=16$. The asymptotic outgoing wave boundary condition is set at $R_m=88$ fm. The results are shown in Figs. 8 and 9. Again, the $a_\gamma^{(+)}(R)$ show rapid convergence for the elastic channel and the *s*-wave ($l=0$) breakup channel $i=4$ and a small slow convergence for the *s*-wave breakup channel $i=16$ near k_m. The ratio $\rho_\gamma(R)$ for the channel $i=16$ is about 0.08 near $R=20$ fm, but in practice this produces only negligible breakup cross sections.

The analysis of $a_\gamma^{(+)}(R)$ and $\rho_\gamma(R)$ indicates (I′) that few incoming waves are little generated at $R\gtrsim 30$ fm which would otherwise be propagate back to the inner region, R

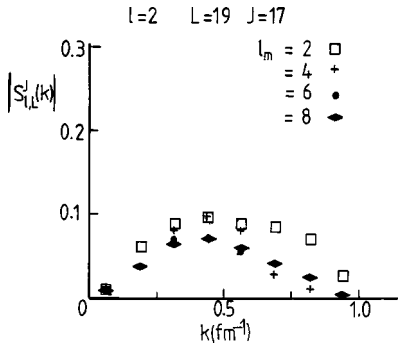

FIG. 5. Discretized breakup *S*-matrix elements to *d*-wave breakup states with $J=17$ and $L=19$. These are calculated by the Av method. Here l_m varies from 0 to 8 through even values, while R_m is fixed at 60 fm. The symbols □, +, ●, and ◇ correspond to $l_m=2$, 4, 6, and 8.

TABLE II. Convergence of the elastic *S*-matrix element with respect to increasing R_m at the grazing angular momentum $J=17$ for the system $d+^{58}$Ni at 80 Mev. Parameters taken are $l_m=6$ fm and $k_m=1$ fm^{-1}. Mid discretization is used with $N=8$.

R_m (fm)	$\lvert S^J_{\rm el}\rvert$	Phase (deg)
30	0.5954	19.9
60	0.5954	19.9
90	0.5954	19.9

$\leqslant R_m$. The reason for this is the smoothness of coupling potentials between breakup channels. Property (I′) guarantees the convergence of the CDCC solution at $R_m=30$ fm. This also means that the coupling potentials between high l breakup channels which dominate at $R>R_m$ do not affect the wave function at $R\leqslant R_m$. This consideration is supported by Fig. 10. The wave function at $R\leqslant R_m$ does not contain high l breakup components, because the coupling potentials to such breakup channels are very weak there. Thus, property (I) guarantees also the convergence of the CDCC solution with respect to increasing l_m. Assuming property (I), the work of Ref. [10] showed that the CDCC solution tends to the exact one as the model space is extended. The present result supports the statement.

V. SUMMARY AND DISCUSSION

We have numerically examined two basic assumptions of the CDCC method, the model space truncation and the discretization of the k continuum, and the practical application of the CDCC method to nuclear reactions involving weakly bound projectiles which can break up easily, either virtually or really, in the course of the reaction. We take $d+^{58}$Ni scattering at 80 MeV as a typical realistic example and carry out numerical tests of the two assumptions. Tests in realistic cases are important since the CDCC method has successfully been used for analyses of experimental data. We have used the Beccheeti-Greenlees nucleon-nucleus optical potentials at half the incident deuteron energy, 40 MeV, throughout the

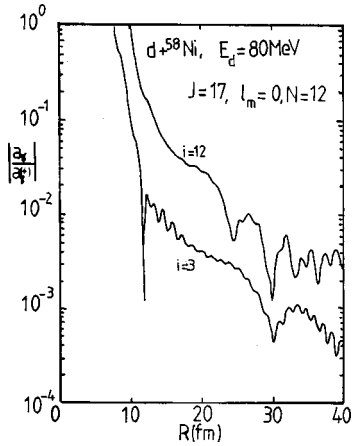

FIG. 6. The ratio $\rho_\gamma(R)=|a_\gamma(R)/a_\gamma^{(+)}(R)|$ calculated with the Mid method. Here γ is taken as $(i,\ l,\ L,\ J)=(i,0,17,17)$ for $i=3$ and 12.

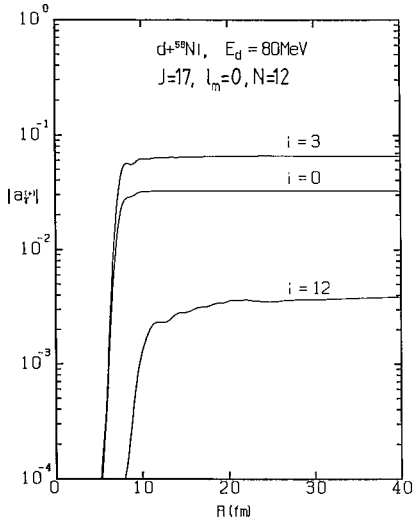

FIG. 7. The amplitude functions $a_\gamma^{(+)}(R)$ calculated with the Mid method. Here γ is taken as $(i, l, L, J)=(i,0,17,17)$ for $i=0$, 3, and 12.

work. As the model space, the internal linear momentum k and the orbital angular momentum l of the n-p pair are truncated at k_m and l_m, and the distance R between the centers of mass of the n-p pair and A at R_m. We have changed l_m up to 8 and R_m up to 90 fm. We have kept k_m fixed at 1 fm since tests for increasing k_m have already been made in detail in Ref. [3].

Av discretization was criticized [4,7] for the reason that the coupling potentials between the discretized breakup channels decay as R^{-4}, whereas the original ones decay as R^{-2}. We have then tested the Av method by comparing it with Mid method which retains the proper asymptotic forms of the original coupling potentials. We have carried out CDCC calculations with the two methods of discretization in the same model space with $l_m=0$, $R_m=30$ fm and looked at convergence of the calculated S-matrix elements with respect to increasing N, the number of discretized breakup channels. We have found that the S-matrix elements converge to the

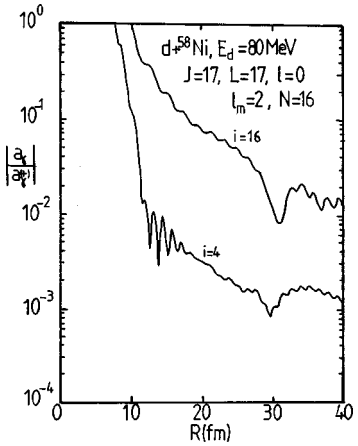

FIG. 8. The ratio $\rho_\gamma(R)=|a_\gamma(R)/a_\gamma^{(+)}(R)|$ calculated with the Mid method. Here γ is taken as $(i, l, L, J)=(i,0,17,17)$ for $i=4$ and 16. Parameters taken are $l_m=2$ and $N=16$.

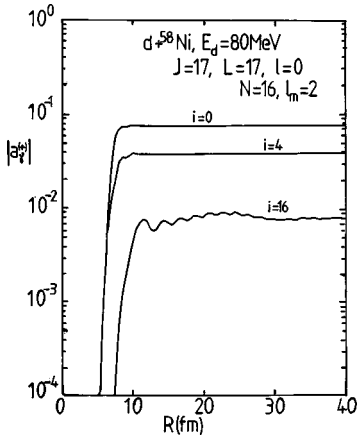

FIG. 9. The amplitude functions $a_\gamma^{(+)}(R)$ calculated with the Mid method. Here γ is taken as $(i, l, L, J)=(i,0,17,17)$ for $i=0$, 4, and 16. Parameters taken are $l_m=2$ and $N=16$.

same values. This clearly shows that the CDCC results are independent of the method of discretization and, consequently, justify the Av method. We have also found that the Av method yields faster convergence and so is more useful in practice than the Mid method.

The validity of the Av method which has short ranged coupling potentials raises a question: What is the role of the long ranged tails of the Mid coupling potentials at $R>R_m$? We have investigated this question through the behavior of $a_\gamma(R)$ and $a_\gamma^{(+)}(R)$ which are related to the channel wave functions as $g_\gamma(\hat{P}_i,R)=a_\gamma(R)f_\gamma(R)+a_\gamma^{(+)}(R)U_\gamma^{(+)}(R)$. If there is any incoming wave at $R>R_m$ other than that in the initial channel, setting the asymptotic outgoing wave boundary condition at $R=R_m$ is not valid. The incoming wave amplitude in a breakup channel γ is proportional to $a_\gamma(R)$. We have found that $a_\gamma(R)$ is very small compared to $a_\gamma^{(+)}(R)$ in the important breakup channels for which the S-matrix elements are large. Even in the breakup channels with small S-matrix elements, the asymptotic outgoing wave

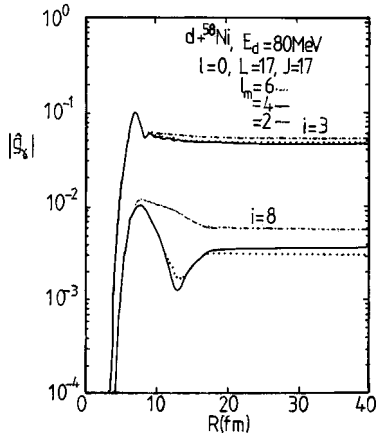

FIG. 10. Breakup channel wave functions $\hat{g}_\gamma$. Here γ is taken as $(i, l, L, J)=(i,0,17,17)$ for $i=3$ and 8. These are calculated by the Av method with $R_m=60$ fm. The dash-dotted and dotted lines correspond to $l_m=2$ and 6, and the solid line corresponds to $l_m=4$.

boundary condition is well satisfied within the accuracy of practical interest. We have extended the same calculation to the larger model space with $l_m=2$ and reached the same conclusion. Thus, long ranged tails of the Mid coupling potentials do not make any essential contribution to the CDCC solution.

The model space truncation is the most essential assumption in the CDCC method, because with this truncation the kernel of the integral equation form of Eq. (2.13) is compact [10]. It consists of three kinds of truncation: (i) truncation of l at l_m, (ii) truncation of k at k_m, and (iii) setting the asymptotic boundary condition at a finite value of R_m. We have tested the truncations (i) and (iii). The test of (ii) has already been made in detail in Ref. [3].

The convergence of elastic and breakup cross sections with respect to l_m was first obtained in Ref. [3] with Av discretization at $l_m=4$ for $k_m=1$ fm^{-1}. It was found that $l_m=2$ was sufficient for elastic scattering cross sections. It was questioned [4], however, if the convergence was not due to Av discretization which alters the asymptotic R dependence of the coupling potentials between continuous breakup states to R^{-4} from the original R^{-2}. We have, therefore, tested the validity of the l truncation with both the Av and Mid method. The Mid coupling potentials between discretized breakup states retain the proper asymptotic form of the original coupling potentials. Their strength at large R increases with l. We have therefore increased both l_m and R_m until the S-matrix elements converge. It is found that the important elastic S-matrix elements converge at $l_m=2$ in both the Av and Mid methods of discretization and independent of R_m for $R_m \geqslant 30$ fm. Breakup S-matrix elements converge in the Av method at $l_m=6$ and $R_m=30$ fm, and only small S-matrix elements are sensitive to R_m. The small elements also converge at $l_m=6$ and $R_m=60$ fm. In the Mid method, the breakup S-matrix elements converge at $l_m=6$ and $R_m=60$ fm, except for small S-matrix elements for which an R_m larger than 60 fm may be needed. However, we do not pursue this possibility any further, because numerical errors due to the integration of coupled differential equations over R larger than 60 fm may not be negligible.

When the S-matrix elements converge with respect to increasing l_m, we have looked at the rate of convergence of the wave functions as l_m increases, and found that the inner parts of the wave functions also converge at $l_m=6$. Coupling potentials between $l>4$ breakup channels do not affect the inner parts of the wave functions, as predicted in Ref. [5].

We have found, from the analyses of $a_\gamma^{(+)}(R)$ and $\rho_\gamma(R)$, (I′), that few incoming waves are generated at $R \gtrsim 30$ fm. This is due to the smoothness of the coupling potentials between breakup channels [14]. This is a necessary and essential condition for the validity of the model space truncation. Property (I) directly guarantees the convergence of the CDCC solution with respect to increasing R_m and justifies truncation of R. Property (I′) also shows that when $R_m>30$ fm, any smooth coupling potentials between breakup channels at $R>R_m$ little reflect the outgoing waves back to the inner region $R \leqslant R_m$, namely, that coupling potentials between high l breakup channels which are important only at $R>R_m$ do not affect the CDCC wave function at $R \leqslant R_m$. The latter, therefore, does not contain the high l breakup components. Thus, property (I) guarantees also the convergence of the CDCC solution with respect to increasing l_m and justifies the truncation of l. According to Ref. [10], furthermore, the CDCC solution Ψ_{CDCC} has an error proportional to $V_{np}\Psi_{\mathrm{CDCC}}$. The interaction $V_{np}(r)$ is a short ranged function of r, so only the very low l components of Ψ_{CDCC} contribute to the error. Obviously, the error vanishes as l_m increases. Thus, the CDCC solution tends to the exact one as the model space is extended, as predicted in Ref. [10].

We have also examined roles of the absorptive part of the optical potentials and found that the absorptive part accelerates the convergence of the CDCC solution, as predicted in Refs. [6] and [10].

In view of all the results described above, we conclude that the two assumptions made in the CDCC method, the model space truncation and the discretization of k continuum, are well justified in the realistic case investigated. The CDCC method, therefore, is well founded as a practical method of calculation to deal with reactions involving weakly bound projectiles such as deuteron, ^{6,7}Li, etc.

ACKNOWLEDGMENTS

This work was supported by a Grant-in-Aid of the Japanese Ministry of Education, Science, Culture and Sports (Monbusho). One of the authors (R.A.D.P.) wishes to thank the Japanese Government for support. The calculations were performed at the Computer Center of Kyushu University under financial support to international collaborations for computational work at the Center.

[1] M. Kamimura, M. Yahiro, Y. Iseri, Y. Sakuragi, H. Kameyama, and M. Kawai, Prog. Theor. Phys. Suppl. **89**, 1 (1986).

[2] N. Austern, Y. Iseri, M. Kamimura, M. Kawai, G. H. Rawitscher, and M. Yahiro, Phys. Rep. **154**, 125 (1987).

[3] M. Yahiro, N. Nakano, Y. Iseri, and M. Kamimura, Prog. Theor. Phys. **67**, 1464 (1982).

[4] T. Sawada and K. Thushima, Prog. Theor. Phys. **76**, 440 (1986).

[5] M. Kawai and M. Yahiro, in *Proceedings of the International Workshop on the Few-Body Approach to Nuclear Reactions in Tandem and Cyclotron Regions*, Tokyo, 1986, edited by S. Oryu and T. Sawada (World Scientific, Singapore, 1987), p. 234.

[6] N. Austern and M. Kawai, Prog. Theor. Phys. **80**, 694 (1988).

[7] T. Sawada and K. Thushima, Prog. Theor. Phys. **79**, 1378 (1988).

[8] R. A. D. Piyadasa, Ph.D thesis, Kyushu University, 1989 (unpublished).

[9] R. A. D. Piyadasa, M. Yahiro, M. Kamimura, and M. Kawai, Prog. Theor. Phys. **81**, 910 (1989).

[10] N. Austern, M. Yahiro, and M. Kawai, Phys. Rev. Lett. **63**, 2649 (1989); N. Austern, M. Kawai, and M. Yahiro, Phys. Rev. C **53**, 314 (1996).
[11] Gy. Bencze and E. F. Redish, Phys. Lett. **91B**, 1 (1980); M. C. Birse and E. F. Redish, Nucl. Phys. **A406**, 149 (1983).
[12] M. Ichimura, M. Igarashi, S. Landowne, C. H. Dasso, B. S. Nilsson, R. A. Brogalia, and A. Winther, Phys. Lett. **67B**, 129 (1977).
[13] F. D. Becchetti, Jr. and G. W. Greenlees, Phys. Rev. **182**, 1190 (1969).
[14] R. Y. Rasonavio and G. H. Rawistscher, Phys. Rev. C **39**, 1709 (1989).